CIRP Journal of Manufacturing Science and Technology 52 (2024) 296–306

Contents lists available at ScienceDirect

CIRP Journal of Manufacturing Science and Technology

journal homepage: www.elsevier.com/locate/cirpj

Non-destructive on-machine inspection of machining-induced deformed layers

Matthew Brown *, Pete Crawforth, David Curtis

University of Sheffield Advanced Manufacturing Research Centre, Wallis Way, Catcliffe, Rotherham S60 5TZ, United Kingdom

ARTICLE INFO

Keywords:
Surface integrity
Non-destructive
Zero defect
On-machine inspection

ABSTRACT

Complete inspection of workpiece surface integrity invariably involves a form of destructive testing to enable the assessment of microstructural defects such as machining-induced white layers and near-surface plastic deformation. The incumbent offline and destructive microscopy inspection process is incompatible with both a digital and sustainable manufacturing vision of zero waste, as such, a non-destructive technique which utilises a novel X-ray diffraction surface integrity inspection method (XRD-SIIM) has been developed. This approach has been designed to complement traditional machinability-type assessments of tool life and machined surface topography, establishing a new process flow for validation. In this paper, for the first time, non-destructive on-machine validation of workpiece microstructural surface integrity is demonstrated, via a comparative investigation into the effect of insert grade, cutting speed and coolant delivery method on the depth of the imparted plastic deformation depth. It is shown that XRD-SIIM allows repeatable, non-destructive determination of deformed layers within a typical machining centre enclosure, with comparable findings to the incumbent cross-sectional microscopy approach. The generation of surface integrity digital fingerprints of a machining operation facilitates rapid comparison between testing variables, with a transition to an objective quantifiable assessment rather than one which open to subjectivity. In turn, XRD-SIIM expedites the development and benchmarking of new operations, tooling, materials, or coolant.

1. Introduction

Benchmarking of new workpiece material, tooling or coolant has historically focused on the balance of tool wear, cutting forces and the surface integrity against material removal rate. Surface integrity encompasses the surface topography, the near-surface microstructural features as well as properties such as microhardness and residual stress state. Whilst tool wear, topography and cutting forces can be obtained on-machine either in-process or post-process [1] and residual stress and microhardness can be obtained on the post-machining non-destructively or with minimal impact on the component, the incumbent process for deformed layer inspection is cross-sectional microscopy, which is inherently destructive. However, the assessment of microstructural surface integrity inspection is a requirement in many industrial applications due to the direct influence of microstructural anomalies on the fatigue performance of a component in service. For example, the formation of features such as machining-induced white layers can reduce low cycle fatigue life by as much as a factor of 10, even after shot-peening, as shown by Herbert et al. [2]. The cutting conditions, tool wear, coolant and material condition of supply can all affect the microstructural surface integrity, particularly in difficult-to-machine alloys with high strength and low thermal conductivity, such as titanium and nickel-based superalloys [3]. Therefore, the assessment of machining-induced deformation depth is an important step in the validation of fatigue-critical components, such as those used in aeroengine applications [4].

It could be argued that tool wear and cutting forces can be used as process indicators of microstructural surface integrity. For example, Bushlya et al. in Inconel-718 [5] and Brown et al. in Ti-6Al-4 V [6] have shown that tool wear assessment can be used as a gauge for the formation of machined surface integrity features such as distorted grains and mechanically induced white layers. However, machining defects can also be generated when cutting with unworn tooling, for example thermally induced white layer formation during machining of steels at high cutting speeds, even when the insert flank wear is smaller than 0.2 mm [7], a common wear limit applied in industry. This observation has been mirrored by Chou and Evans [8]. Cutting forces can also be linked to defect generation with previous research having associated high

* Corresponding author.
E-mail address: m.o.brown@amrc.co.uk (M. Brown).

https://doi.org/10.1016/j.cirpj.2024.06.006
Received 27 March 2024; Received in revised form 23 May 2024; Accepted 11 June 2024
Available online 25 June 2024

compressive (thrust) forces with the formation of a white layer via a severe plastic deformation mechanism, for example when milling Ti-6Al-4 V [6] or hard turning of steel [8] both with worn tooling. However, the same methodology cannot be applied when a white layer is generated via the thermal mechanism.

Despite their application as process indicators, tool wear assessment and cutting force measurement are not a direct test of workpiece microstructural surface integrity, yet a level of near-surface plastic deformation of the workpiece is present to varying severity in all chip-forming machining processes. This is due to the mechanics of chip formation in which the primary deformation zone extends below the depth of cut with a transition region into the tertiary shear zone beneath the tool, as illustrated by Uysal et al. [9]. As such it is important to be able to measure defects such as near-surface deformation directly rather than infer it from process indicators.

Current methods for benchmarking machined surfaces during new product or process development are limited in terms of the microstructural surface integrity information that can be obtained without the need to preserve numerous specimens for cross-sectional microscopy inspection. Incumbent methods are also limited by the part coverage as microscopy is a 2D plane assessment so can only capture defects on a small plane, rather than over an area. Microscopy is typically reliant on interpretation via an inspector, which therefore introduces a level of subjectivity to the assessment. Whilst automated vision inspection of micrographs could remove some of this subjectivity, the variation in micrographs even for a single alloy due to etch response as well surface preparation differences may prove challenging for a vision system. An additional factor to consider is the long lead time for results, due to the requirement for sectioning and the numerous cross-sectional specimen preparation steps required before microscopy, which can bottleneck the iterative design process. However, the recent development of a novel non-destructive X-ray diffraction surface integrity inspection method (XRD-SIIM) [10] means it is now possible to non-destructively detect and size fatigue-limiting microstructural features.

XRD-SIIM can be applied to inspect for microstructural features such as machining-induced white layers and regions of grain distortion (distorted layers) in which the microstructure is deformed in the cutting direction [11]. The technique utilises the phenomenon of diffraction peak broadening caused by small crystallite size (grains or sub-grains) and inhomogeneous lattice strain arising due to imperfections in the crystal lattice, for example due to a high dislocation density [12]. The defect classification criteria and sizing models are trained using reference samples in the material of interest with known microstructural surface integrity. In previous work by Brown et al. [10,11] and Naskar and Paul [13], an increase in the full width at half maximum (FWHM) has been associated with increased deformed layer thickness or the presence of a white layer. However, for white layers a contrasting observation was recorded by Kwong et al. [14] in a drilled hole, suggesting that temperature effects may be leading to a level of dynamic recovery in the crystal lattice during white layer formation, reflected by a reduction in XRD peak breadth.

Historically, diffraction peak breadth calculated from the FWHM value has been used as a measure of grain size and plastic strain levels in a material [15], alongside complementary data obtained from methods such as scanning electron microscopy. For example, Baumann et al. [16] estimated the grain size in a white layer formed on a worn rail track using X-ray diffraction (XRD) peak broadening, however conventional lab-based diffractometers necessitate destructive sectioning of real engineering components to fit within the confines of the diffractometer. With the availability of modern portable diffractometers, designed with inspection of real components in mind, the use of XRD as a non-destructive method for deformed layer assessment within a typical machining environment is now realisable.

Due to an increasing drive towards sustainable manufacturing, to meet global net zero emissions by 2050 and avoid the worst impacts of climate change [17], the manufacturing industry must improve machined component quality to reduce waste. This encompasses a reduction in energy and physical waste such as scrap components, as well as to extension to the product life-cycle offered by component assurance. In the manufacture of high-value aerospace components, current inspection methods are often lab-based and in some cases destructive, so represent a clear area for improvements towards manufacturing sustainability. If sustainable manufacturing is to be achieved, defects must be predicted and detected on-machine, such that corrective action can be taken, rather than wasting significant energy and resources continuing to make components which ultimately fail inspection. This forms the basis of zero defect manufacturing, as outlined by Powell et al. [18]. This approach also offers a digital fingerprint of potential life-limiting sub-surface defects, which can support a longer-in-use philosophy which is a further aspect of sustainability, beyond the initial manufacturing stage. This information could feed into the digital passport of a component, encompassing the data associated with a component from across its lifecycle. This in turn may ultimately be used to support a simulation-based digital twin that predicts the measured phenomenon.

Through the utilisation of X-ray diffraction surface integrity assessment, it is proposed that the deployment of new subtractive manufacturing processing routes can be accelerated due to the information XRD-SIIM can rapidly provide about the influence of different test variables on the microstructural surface integrity. Whilst the technique is not currently accredited due to its novelty, the process can be used in a research and development environment to reduce the number of assessments required from incumbent destructive methods thereby improving material efficiency. This study aims to expand on the previous work by Brown et al. [10,11] where XRD-SIIM has been validated against the incumbent microscopy process for machining deformation assessment, to investigate the capability for on-machine microstructural surface integrity inspection with XRD-SIIM. The focus of the study is to present the XRD-SIIM approach to machining process optimisation and demonstrate its effectiveness as a supporting process optimisation tool when compared to the incumbent microscopy approach, not to evaluate which specific combination of process parameters gives the optimal surface.

2. Experimental methodology

To investigate the effectiveness of XRD-SIIM as a process development tool, tool life tests were undertaken by face turning RR1000 nickel-based superalloy workpiece using a Mori-Seiki NMV8000 5-axis machining centre. This experiment was designed to evaluate the effect of changing common machining variables such as the cutting conditions, insert grade and coolant application method on the microstructural surface integrity, using the novel on-machine XRD-SIIM method. Based on the XRD-SIIM assessment, preferential machining operations could be down-selected for further testing, as would typically occur over a much longer time scale during traditional process development where microscopy is used. The various tests and corresponding down-selection steps undertaken in this study, which were selected to represent a typical set of machining process development trials, are illustrated in the diagram in Fig. 1. The focus of the study is to present the XRD-SIIM approach to machining process optimisation and demonstrate its effectiveness when compared to the incumbent approach, not to evaluate which cutting conditions give the optimum surface, as this will depend on the specific limits imposed by the component life cycle. As such the cutting speeds and feed rates have been normalised with respect to one of the material removal rate conditions tested, which was defined as 100 % cutting speed and 100 % feed rate. A 0.25 mm depth of cut was used throughout the study to represent a typical value for a finishing operation.

Previous work on XRD-SIIM [11] has been limited to lab-based non-destructive inspection of machined components off-machine or pseudo-non-destructive assessment of coupons extracted for microscopy

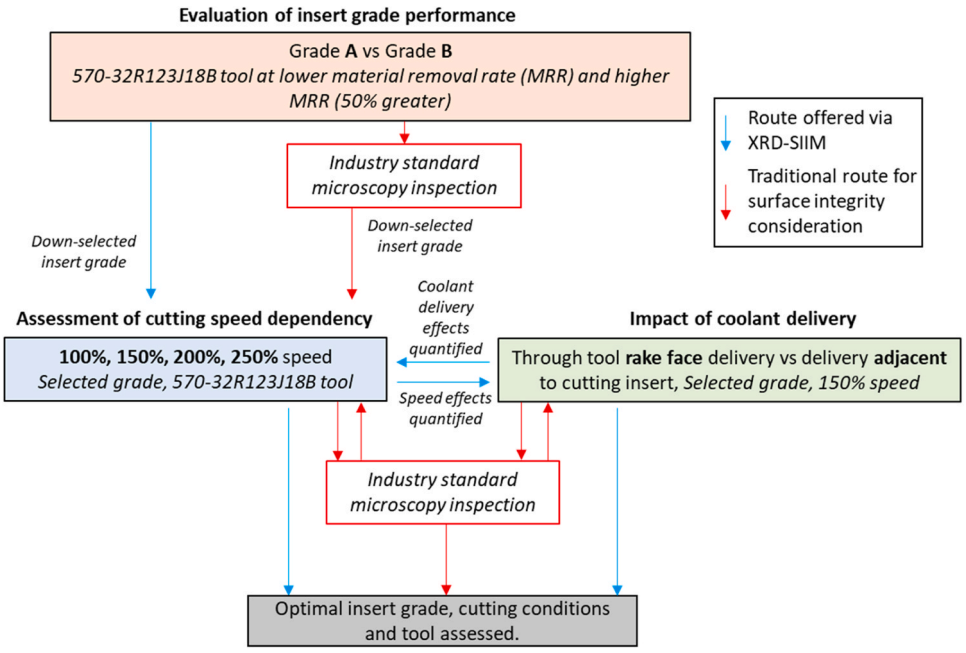

Fig. 1. A diagram illustrating the process flow for a series of trials for machining process development, using XRD-SIIM (blue) and industry-standard microscopy inspection (red).

validation. This study brings, for the first time, XRD-SIIM inspection out of the laboratory environment, onto the shop floor, to enable the expedited machining process development trials as outlined in Fig. 1. Earlier studies focused on the validation of XRD as a method for deformed layer inspection against the microscopy process. This study therefore seeks to apply the technique to a real-world research and development challenge to investigate the improvements it can bring to such activities compared to the traditional approach.

The procedure for XRD-SIIM has been introduced in detail previously [11] but is summarised in the diagram in Fig. 2. First, a diffraction pattern of the peak of interest is captured and then the FWHM peak breadth is extracted from the data. The measured FWHM value is then passed through a model, which describes the dependence of peak breadth on the depth of machining-induced deformation in the alloy being inspected, to assess deformed layer thickness. This model is derived from diffraction theory and is calibrated using machined test pieces with a layer thickness that has been quantified through conventional microscopy assessment, as outlined by Brown et al. [11]. Metallurgical preparation for these calibration specimens was achieved by grinding with successively finer grinding papers P800-P2500 before polishing with 1 μm colloidal silica suspension and etching with Kalling's reagent. Micrographs at 1000x magnification were obtained and the depth of deformation was quantified as the average perceived depth of deformed grain structure across three locations on each specimen, a comparable methodology to that applied in industry.

Validation measurements reported in the earlier study [11] showed a defect layer sizing accuracy of under 2 μm when comparing XRD-SIIM to microscopy, for layers up to the X-ray penetration depth (14 μm). Beyond the X-ray penetration depth, the technique loses sizing resolution and there is reduced confidence in distinguishing, for example, between a 40 μm layer and a 45 μm layer. However, XRD-SIIM is still able to identify both instances, qualitatively, as heavily deformed. For machined surfaces with good microstructural surface integrity, defect layer thicknesses below 15 μm would be expected for typical materials so as such, XRD-SIIM has good sensitivity over a relevant range for microstructural surface integrity assurance.

During the trials, two different chemical vapour deposition grades of Sandvik Coromant carbide cutting insert were tested, using identical N123J2–0600RO geometries. Both inserts (anonymised to A and B here) have the same tungsten carbide substrate with the same chemical vapour deposition coating applied by two different methods as coating technology is constantly evolving. These inserts were held in one of three types of tools to investigate the effect of coolant delivery on deformed layer thickness. A 570–32R123J18B tool with through-tool coolant directed to the side of the insert in the path of the cutting tool, a SL70-L123H30A-HP tool with through-tool coolant delivered to the insert rake face and nose radius via a single nozzle and a SL70 R123K15-HP tool with through tool coolant delivered via three jets to the rake face and nose radius.

Hocut 4260 at a concentration of 6.5 %−7.5 % delivered at 45 bar was used as the coolant during turning. Trials were performed with a radial length of cut between 10 mm and 16.5 mm with the value used

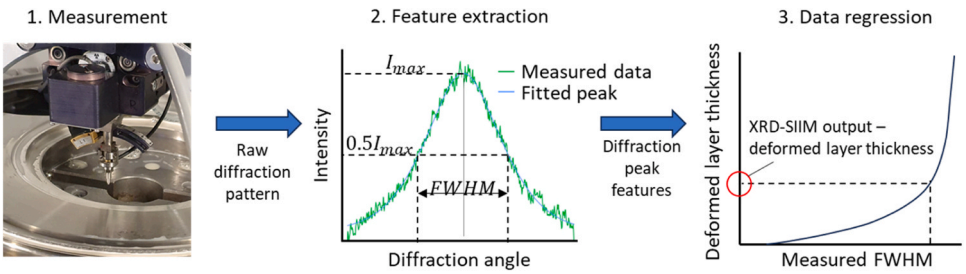

Fig. 2. A diagram of the XRD-SIIM measurement, extraction, and regression procedure.

being a function of the diameter at which the cut was being performed, to ensure the spiral length of cut was kept constant. The small radial length of each cut was chosen to allow XRD-SIIM and tool wear inspection at regular short intervals. For each trial, XRD-SIIM inspection was performed for the first two to three tool passes, with the inspection interval increased after that point and then adjusted based on the rate of progression of tool wear or XRD-SIIM measured deformation. For example, if a significant change from the previous inspection was recorded, then the inspection intervals were shortened. A 45° chamfer was created on the engagement tool path for tool entry to prevent the insert from notching. An additional set of tool wear tests were performed with an increased radial length of cut to reduce the number of tool entries over the life of the tool. This was undertaken to validate the assumption that the shorter cuts used in much of this study, to facilitate shorter XRD-SIIM and tool wear assessment intervals, were not affecting the results due to the increased number of entries into cut. Details of the machining trials performed are outlined in Table 1.

On-machine XRD-SIIM was undertaken using a Proto iXRD portable residual stress diffractometer mounted to a wheeled support structure, as shown in Fig. 3(a), to allow the diffraction head to be brought up to the workpiece for inspection, as illustrated in Fig. 3(b). The XRD system was removed from the machining centre before the next machining step. Manganese X-ray radiation was used at a voltage of 20 kV and a current of 4 mA to capture a diffraction pattern for the (311) face centred cubic crystallographic plane at a diffraction angle of approximately 154°. The broadening of X-ray diffraction peaks, which arises from inhomogeneous lattice strain [19] and crystallite size [20] effects, increases with diffraction angle. It is, therefore, important to select an X-ray radiation type which places the diffraction peak at a high angle and maximises the peak broadening effects. The (311) peak was used as Brown et al. [11] have shown that this high-angle peak is sensitive to machining-induced damage. It was measured, from XRD-SIIM tests on surfaces on which metalworking fluid was present, that whilst the elemental composition of the coolant does not give rise to additional diffraction peaks in the region of interest or X-ray fluorescence, the fluid acts as an X-ray attenuator. This reduces the intensity of the X-ray beam which reaches the workpiece therefore, residual coolant from the previous machining pass was wiped away before XRD-SIIM measurements.

Table 1
Details of the machining trials undertaken.

Trial	Purpose	Insert grade	Cutting speed	Coolant delivery	Depth of cut (mm)	Feed rate
I	Grade A vs Grade B	A	100 %	Through tool adjacent	0.25	133 %
II	Grade A vs Grade B	B	100 %	Through tool adjacent	0.25	133 %
III	Grade A vs Grade B	A	85 %	Through tool adjacent	0.25	100 %
IV	Grade A vs Grade B	B	85 %	Through tool adjacent	0.25	100 %
V	Cutting speed dependency	A	150 %	Through tool adjacent	0.25	133 %
VI	Cutting speed dependency	A	200 %	Through tool adjacent	0.25	133 %
VII	Cutting speed dependency	A	250 %	Through tool adjacent	0.25	133 %
VIII	Coolant delivery	A	150 %	1 nozzle to rake face	0.25	133 %
IX	Coolant delivery	A	150 %	3 nozzles to rake face	0.25	133 %
X	Repeatability 1	A	55 %	Through tool adjacent	0.25	100 %
XI	Repeatability 1	A	55 %	Through tool adjacent	0.25	100 %
XII	Repeatability 2	A	85 %	Through tool adjacent	0.25	100 %

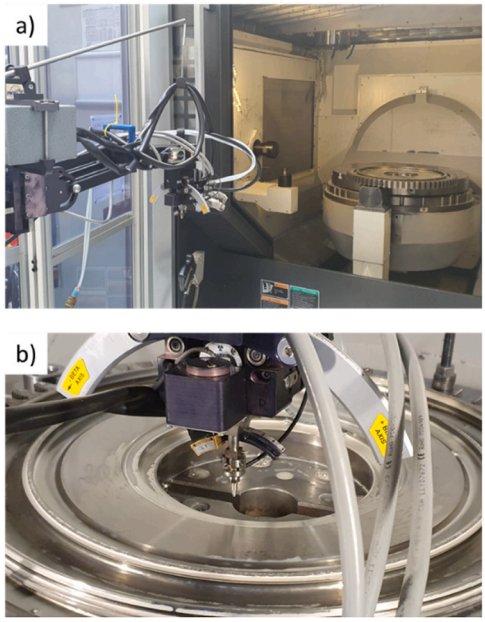

Fig. 3. Photographs of the on-machine XRD-SIIM hardware arrangement. (a) The Proto iXRD head mounted to a wheeled support structure adjacent to the Mori-Seiki NVM8000 and (b) the Proto iXRD head positioned over the RR1000 workpiece during the focusing step.

During the XRD-SIIM measurements, an exposure time of 4 s was used with three exposures per measurement and three full repeats per measurement location. A rectangular 1 mm × 5 mm beam aperture was used to control beam divergence, with the measurement taken in the central region of the face turned shoulder and the long axis of the aperture aligned to the radial direction. The measurement was performed with the incident X-ray beam perpendicular to the specimen. Only a single inspection orientation is required for peak breadth assessment, unlike residual stress assessment which relies on multiple tilt angles. X-ray penetration depth [21] for 95 % attenuation was calculated to be 14 μm. This was obtained using a mass attenuation coefficient (129.1 cm^2/g) calculated from elemental the composition of the alloy and the Mn X-ray radiation used [22], the density of the alloy (8.15 g/cm^3), and the diffraction angle (154°). After each machining step, the workpiece was rotated to the same C-axis position to block the effects of any spatial variation in surface integrity which could arise due to inhomogeneities in the workpiece from prior processing. The XRD pattern was corrected for background intensity via a gain measurement. A pattern was obtained from a ferritic steel specimen with no diffraction peak in the angle range of interest and this was subtracted from the diffraction pattern in the nickel superalloy workpiece. FWHM was obtained from a pseudo-Voigt profile fitted to the measured diffraction peak.

Tool flank wear was measured using a Zeiss Discovery.V8 optical microscope whenever an XRD-SIIM assessment was taken. Flank wear was recorded as the average of three measurements across the width of the flank wear land. To compare XRD-SIIM against the incumbent start and end-of-cut microscopy assessment approach, cross-sectional microscopy specimens representing the start and end of tool life were

extracted and prepared via the metallographic procedures highlighted previously for the calibration specimens, before being imaged with a Nikon LV150NL microscope. Microscopy-measured deformation depth was taken as the average depth of perceived microstructural deformation from three micrographs across each specimen. This was used to validate the deformed layer thicknesses, as would be typically performed using the standard machined surface validation approach in industry. The specimens were taken from the central region of the face turned shoulder, and as such represent a 2D slice within the XRD-SIIM illumination area. This is illustrated in Fig. 4. Note that the validation of XRD-SIIM for microstructural surface integrity assessment has already been reported in previous work in the same nickel-based superalloy [11], therefore, microscopy specimens were not preserved at the tool wear and XRD-SIIM measurement intervals to minimise material waste.

To facilitate a microstructural surface integrity-based comparison of different operations, XRD-SIIM fingerprints were used. These are plots in which the XRD-SIIM measured FWHM, obtained at intervals throughout the cutting operation, have been converted into deformed layer thickness assessments via the physics-based XRD-SIIM model for RR1000. By plotting the tool wear on the same dual y-axis plot as the deformed layer thickness measurements, the XRD-SIIM fingerprint thereby highlights the simultaneous progression of deformed layer thickness and tool wear throughout an operation, facilitating simple comparisons.

When benchmarking different operations, the following rules were applied to highlight how XRD-SIIM could be applied as a process development tool. Note that these rules are not representative of any specific industrial application but illustrate typical factors which might be included as assessment criteria in a range of applications.

1. A desirable operation maintains a consistent thickness of deformed layer throughout the main portion of tool life i.e., a stable operation improves confidence in the microstructural surface integrity.
2. A desirable operation should possess low levels of grain deformation, however, some level of deformation is to be expected in all chip-forming machining operations. As such, in this study, a value above 15 μm was considered excessive, purely to benchmark different operations. Please note this value was selected arbitrarily to demonstrate the applicability of the XRD-SIIM method to an inspection challenge and should not be taken as representative of any surface integrity criteria imposed in industry.
3. When multiple operations meet the other criteria, the operation with an increased material removal rate is considered the most desirable.

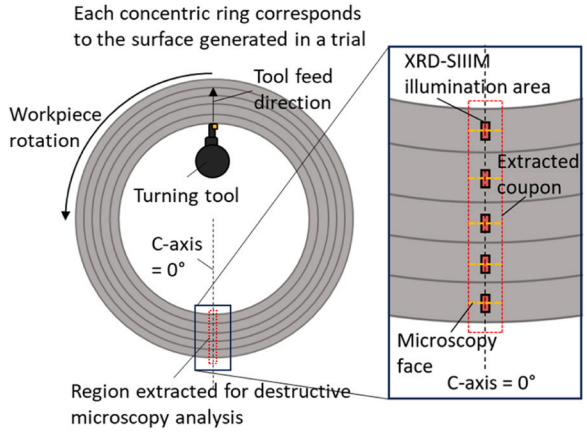

Fig. 4. A schematic of the location of the inspection regions for microscopy and XRD-SIIM on the RR1000 workpiece in relation to the face turning operation. The microscopy face is parallel to the machining direction such that deformation depth can be assessed.

3. Results

In this section the results from the application of XRD-SIIM to a machining process design problem are presented, following the experimental structure outlined previously in Fig. 1.

3.1. Evaluation of insert grade performance

To evaluate the microstructural surface integrity influence of insert grades A and B for the application of nickel workpiece machining, cutting trials were performed at two cutting conditions, one representing a more conservative, lower material removal rate (MRR), set of parameters and the other at 15 % increased cutting speed and 33 % increased feed rate, representing higher material rate cutting conditions that are desirable from a productivity perspective. The XRD-SIIM fingerprints flank wear profiles throughout the tool life tests and a selection of associated cross-sectional micrographs from start and end of tool life specimens are shown in Fig. 5(a-c). Surfaces with a deformation depth greater than 30 μm are represented by a marker on the plot at 30 μm with an arrow extending upwards, this was due to the desire to preserve a Y-axis scale which allowed visualisation of the differences between tests at low deformation levels which are more typical for tool wear levels below 0.2 mm.

At the lower MRR cutting condition, it can be seen from the non-destructive XRD-SIIM measurements in Fig. 5(a) that both insert grades produce a surface with levels of deformation beneath 10 μm, with slightly lower depth values for insert B across the full time in cut. At higher MRR rates, insert A performs better in terms of deformed layer thickness, compared to insert B. Whilst both grades resulted in increased near-surface deformation compared to the trials at lower MRR, insert B produces a significantly worse surface, as deformation reaches 20 μm after just 3.5 min in cut, despite the associated tool wear being within normal acceptable levels of wear. This observation suggests there are additional factors affecting surface integrity beyond those directly attributable to tool flank wear. For insert A, deformation depth remains stable at around 10 μm up until the point at which the tool wear rapidly starts to increase. This stable microstructural surface integrity behaviour up to the onset of significant tool wear is a desirable feature of the turning operation.

Tool wear behaviour for the four trials, as shown in Fig. 5(b), was comparable up to 7 min in cut, at which point insert A at higher MRR and insert B at lower MRR begin to rapidly wear whereas the other two cuts do not exhibit a transition to accelerated wear rates within the tool life tested. Micrographs from the start and end of tool life provide comparable observations to XRD-SIIM at these edge cases but cannot provide assurance throughout tool life without preserving many specimens for cut-ups, which would sacrifice a significant proportion of the available surface area for inspection. As a reminder, each tool pass used a radial length of cut of 10.5–16 mm which would necessitate preservation of a minimum of over 150 mm of radial length of material over just one tool life test, which was more than the available in the workpiece.

From this initial investigation, insert A was taken forward, due to its improved microstructural surface integrity behaviour throughout tool life when compared to insert B at a higher MRR. It is important to note that without microstructural surface integrity inspection throughout these trials, enabled by XRD-SIIM, both grades would appear to give similar results. Tool wear progression and microstructural cut-up assessment from the start and end of cut yielded comparable results across the tests. Ultimately XRD-SIIM was able to provide additional information on performance during the cut enabling insert A to be selected for further tests, over insert B, due to its improved deformed layer thickness performance at a higher MRR.

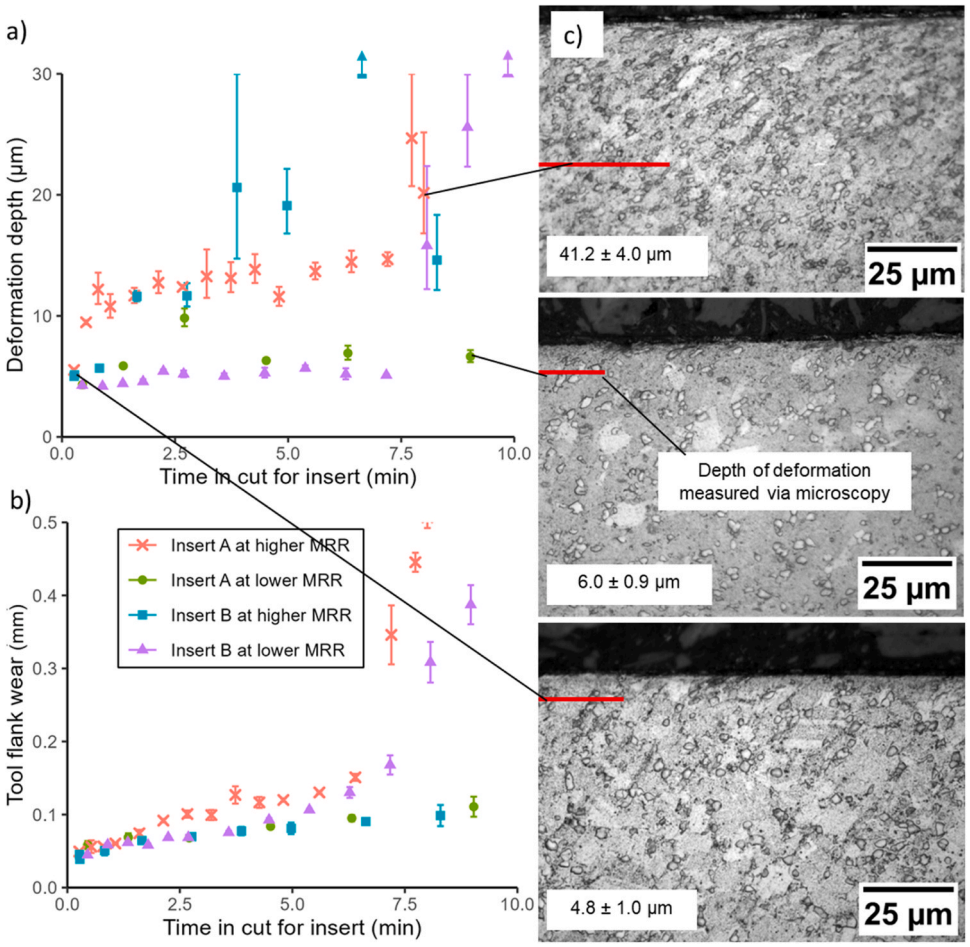

Fig. 5. Plots from the tool life tests (Trial I-IV) showing (a) the XRD-SIIM fingerprints, (b) cross-sectional micrographs of a subset of surfaces and (c) the flank wear profiles throughout each of the four trials. Tool type 570–32R123J18B was used for all trials.

3.2. Assessment of cutting speed dependency

To investigate the effect of cutting speed on the microstructural surface integrity throughout tool life, further trials were performed at speeds corresponding to a range between 100 % and 250 % of a representative baseline cutting speed, in intervals of 50 %. The baseline value was selected as a conservative low speed value which had successfully been used to generate a good surface integrity in earlier testing. All tests were performed with the same feed rate and depth of cut. The deformation depth measured throughout each cut via XRD-SIIM is presented in Fig. 6 alongside the tool wear profiles. Due to the large differences in the time in cut between the tests arising from the differences in cutting

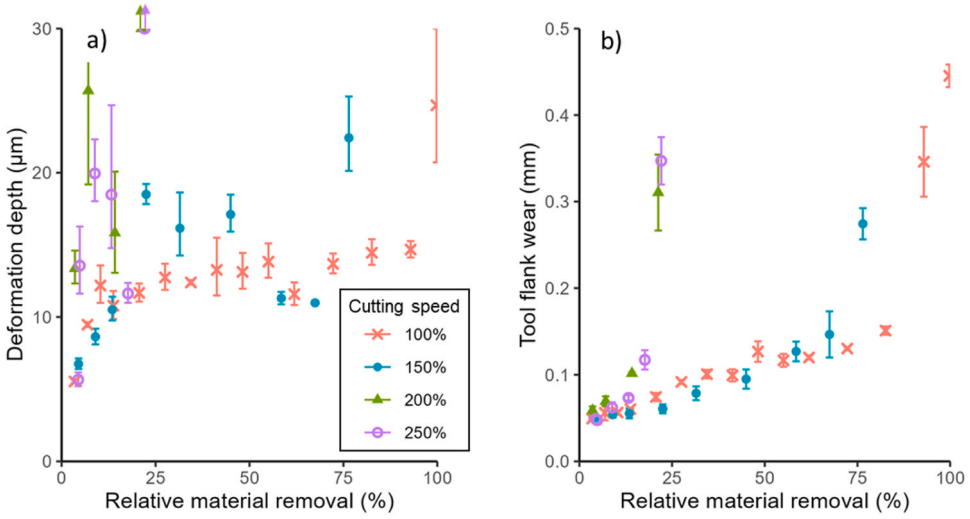

Fig. 6. Plots showing a) the XRD-SIIM fingerprints for different cutting speeds and (b) the corresponding tool flank wear profiles for each test in the cutting speed investigation (Trials I and V-VII).

speed, the results have been plotted against the relative material removal (RMR), normalised against the trial which gave the largest value.

When increasing the cutting speed from 100 % to 150 %, the deformation depth was comparable for the first portion of the cut but after reaching 25 % RMR, the 150 % speed condition was measured to deviate from the lower speed condition with increased deformation depths. The surface deformation for the 150 % condition deteriorates significantly when progressing beyond 75 % RMR, alongside a sudden increase in flank wear. For the 200 % and 250 % cutting speed trials, deformation depth exceeds 15 μm within the first three passes at just 5 % RMR and remains high even at low levels of tool wear. The tool eventually fractured after just 75 % RMR. The XRD-SIIM and tool wear results clearly show that the higher speed conditions perform poorly from both a deformed layer thickness and tool wear point of view. For the 150 % speed condition, tool life when considering material removal, rather than time in cut, is slightly shorter than the 100 % speed condition. When factoring in the extra information provided by XRD-SIIM, which shows increased deformation at 150 % speed, the lowest speed condition performed best overall.

3.3. Impact of coolant delivery

In a parallel investigation, the effect of the coolant delivery method on the deformed layer thickness was evaluated through trials with the three different tooling options, using the same cutting conditions in each test. The conditions used correspond to the 150 % cutting speed parameters used in the cutting speed investigation. The results are shown in Fig. 7(a-c). XRD-SIIM assessment highlights the comparatively poor performance when using the through-tool coolant delivery adjacent to the insert, with increased levels of deformation, even when the tool wear is low at the start of cutting. By contrast, through-tool coolant delivery to the rake face gives comparable microstructural deformation, when using one or three nozzles, with low levels of deformation measured via both XRD-SIIM and microscopy, as presented in Fig. 7(c), for the point at which the trials were halted. The close alignment (2 μm) between XRD-SIIM and microscopy results for thin layers, i.e. those thinner than the X-ray penetration depth as well as the significantly reduced sizing accuracy for thick layers aligns with previous validation work [11].

By cross-referencing the XRD-SIIM fingerprint against the associated tool wear profiles in Fig. 7(b), the 570–32R123J18B tool gave shorter tool life with significant wear after just 4 min in cut. At all points along the tool life plot, the adjacent coolant delivery resulted in higher flank wear compared to the rake face delivery options, however, the tool wear is only 25 % larger up to 2 min in cut. For this early stage in the tool life, XRD-SIIM results show that deformation depth was larger for the 570–32R123J18B tool, and when tool wear reached the same level for the other two tools after 2 min in cut, their resultant surfaces possessed lower deformation depth. This suggests that coolant delivery is influencing the deformed layer thickness directly, rather than having a secondary influence via accelerated tool wear rates.

Diagnosis of the underlying mechanics behind the reduction in

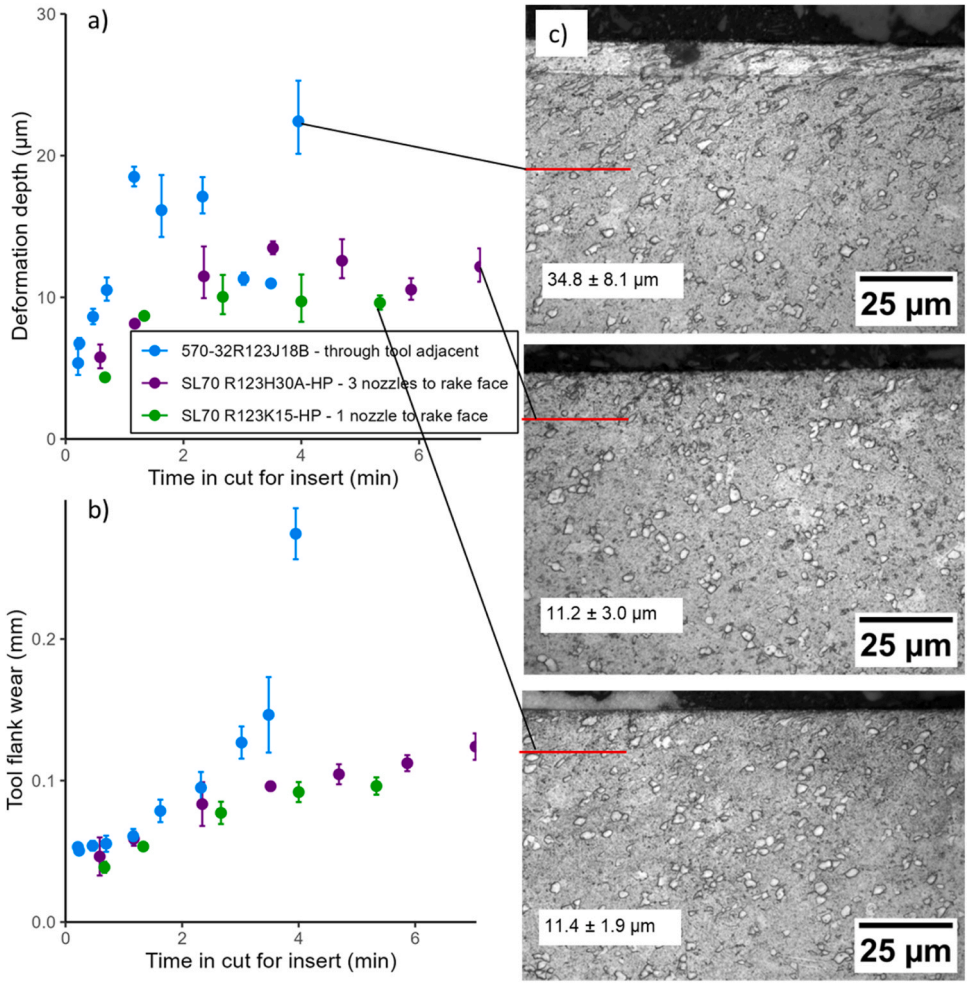

Fig. 7. Plots from the coolant delivery tests showing (a) the XRD-SIIM fingerprints, (b) the associated micrographs from end-of-cut specimens and (c) the flank wear profiles throughout each of the three tests (Trial V, VIII and IX).

deformation with coolant directed towards the insert rake face is not possible without further investigation. This is due to the complexity of the inter-relationships between the heat being generated in the deformation zones and any associated thermal softening or work hardening as well as the low thermal conductivity, high resistance to plastic deformation and strain rate sensitivity of nickel superalloys [23]. However, the application of coolant directly to the rake face using the tools with appropriate through-tool coolant delivery nozzles could improve the cooling of the cutting zone which could result in improved microstructural surface integrity.

The reduction in deformed layer thickness when using the tool with adjacent delivery, between 2 and 4 min in cut cannot be explained by the flank wear progression, which continues to increase gradually throughout this period. Instead, this could be due to the change in the cutting edge condition, for example, the changes to the cutting edge radius due to concurrent rake and flank wear or fracture of the cutting edge. Future studies should aim to quantify the tool condition, beyond just the flank wear, as well as measure any fluctuation in coolant delivery to identify the cause of the fluctuations in deformed layer thickness. Evidently, assessment of flank wear progression can only be used to infer machined surface condition, and this fails to account for other tool wear metrics such as edge rounding and fracture as well as wear on the rake face. In contrast, XRD-SIIM, as a direct surface integrity assessment method was able to identify a decrease in the deformed layer being generated, flagging that something about the cutting operation has changed compared to the previous surfaces generated.

From the XRD-SIIM and tool wear fingerprints it is readily apparent that the through-tool, one and three nozzle tool holders with rake face delivery give optimal microstructural surface integrity performance, as such either of these solutions represents the optimal tooling solution in this study. The 150 % speed and rake-face coolant delivery operation has been compared against the 100 % and 150 % speed operations with non-optimal coolant delivery in Fig. 8(a) and (b). The higher speed condition with rake face coolant delivery results in the lowest deformation depths throughout the cut and the deformation depth remains stable throughout tool life. When considering the higher metal removal rate afforded by the higher speed condition in addition to the reduced deformed layer thickness, this operation can be identified as the optimal operation when balancing sub-surface condition and productivity. The resulting deformation depth can be accommodated within the 15 μm illustrative deformation limits imposed in this study. The process flow through the various down-selection steps is illustrated in Fig. 9.

3.4. Low speed repeatability

To assess the repeatability of the on-machine XRD-SIIM method, two additional trials were performed over the same radial range on the RR1000 workpiece with two repeats per trial. Arbitrary cutting conditions, coolant delivery and insert grade options were selected for these cuts as the focus was on the repeatability of XRD-SIIM fingerprinting, rather than the effect of process parameters. New inserts were used in both trials. It can be seen from the plot in Fig. 10 (a), that both repeats of test 1 exhibited very similar results with deformation depths within 1 μm between repeats for all measurements up to the point at which tool wear accelerated after 7.5 min in cut. The tool wear progression, shown in Fig. 10 (b), follows the same trend between the repeats. In test 2 there was a greater discrepancy between deformation depth measurements taken at comparable values for the time in cut, however, the general trend across the tool life was comparable. In both repeats of test 2, tool wear gradually increased up to approximately 135 μm after 16 min in cut, with deformation depth between 4–8 μm throughout, aside from an isolated incident of increased deformation level in both trials after approximately 6–7 min of tool life.

The XRD-SIIM method has shown a correlation to within 2 μm of the deformed layer thickness validated with microscopy, for features up to the X-ray penetration depth in this study and in previously published research [11], and all but one surface assessed in the repeatability study had deformation less than the 14 μm X-ray penetration depth. As such it is more likely that the random aspects of tool wear progression in combination and the material response to machining is the primary source of the observed variation between repeats in test 2, instead of the XRD-SIIM method. This is evidenced in Fig. 10 (a) by the comparatively small uncertainties in the XRD-SIIM assessment compared to the deformation depth variation across the tool life test.

4. Discussion

XRD-SIIM inspection in the current iteration of on-machine inspection takes approximately 5 min per measurement, with much of this time required for movement and positioning of the XRD unit, rather than acquiring the measurement, which takes approximately 15 s. This could be lowered further via integration of XRD-SIIM within the machining centre, to facilitate a doors-closed inspection process utilising the machine tool CNC control for positional movement. With a system designed specifically for surface integrity inspection, total measurement time could be brought under 30 s. Microscopy inspection, by contrast

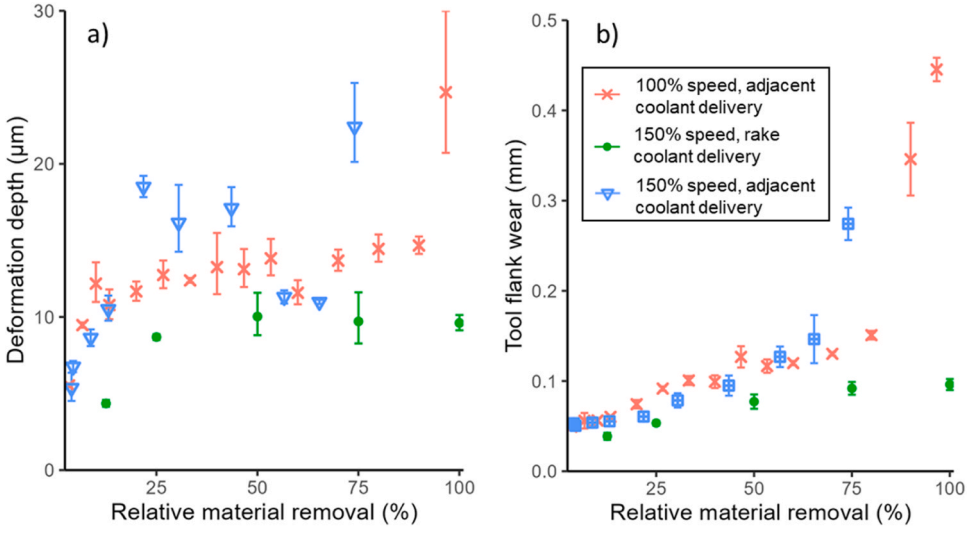

Fig. 8. Plots for the two best performing operations (100 % speed, adjacent coolant delivery and 150 % speed rake face coolant delivery) showing (a) the XRD-SIIM fingerprints and (b) the corresponding flank wear profiles. Trials I, V and VIII.

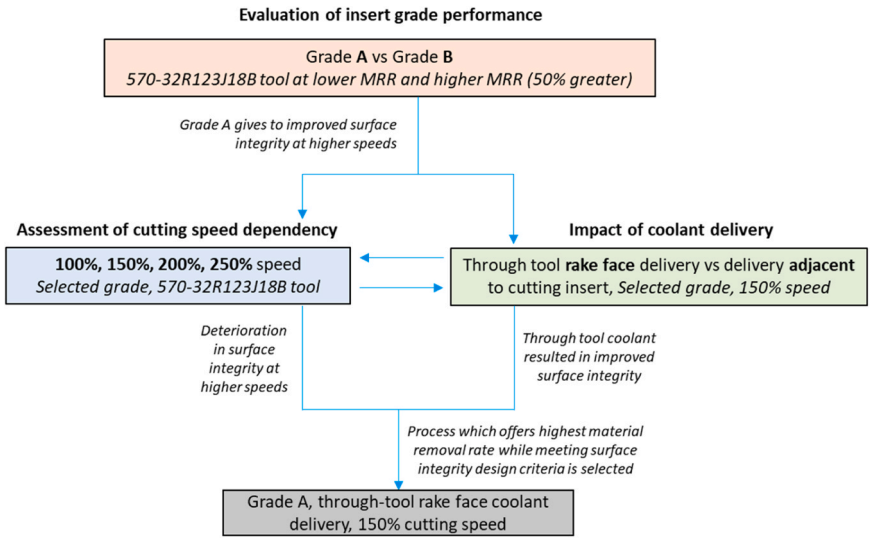

Fig. 9. A diagram illustrating the specific process flow for this application of XRD-SIIM as a process development tool.

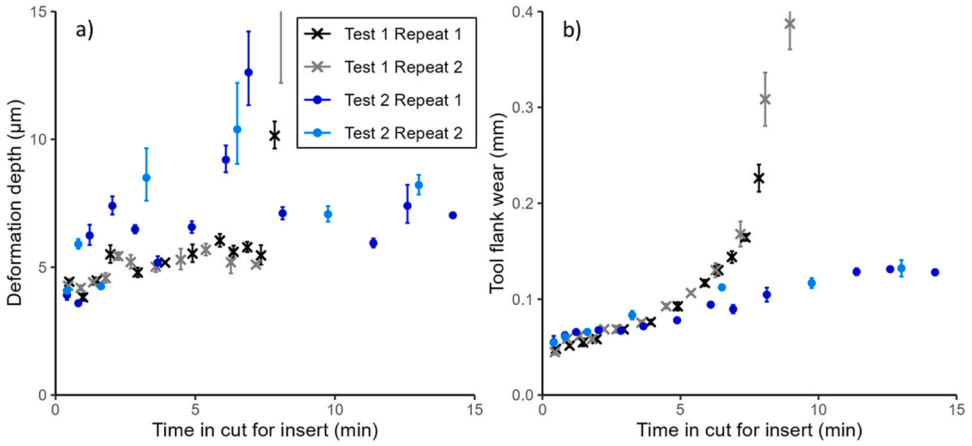

Fig. 10. Plots for two trials each with two repeats (Trial X and XI as well as Trial III and XIII) showing (a) the XRD-SIIM fingerprints and (b) the corresponding flank wear profiles.

typically requires significantly longer due to the need to section, prepare, and then image the microscopy specimens. In most cases these steps are performed in different locations away from the machining centre used to create the machined surface being inspected, which can lead to lead times of days or longer.

The penetration depth of X-rays is both a limitation and strength of the XRD-SIIM technique. It allows XRD-SIIM to be sensitive to thin surface layers, for example, the detection of a white layer thinner than 2 µm, as shown previously [11], but also reduces the sensitivity to deformed layers, e.g. those beyond 20 µm. In industry, processing windows for fatigue-limited aerospace alloy machining are used, however, there is no universal allowable deformed layer depth, as different applications and manufacturers define bespoke levels. The distinction between a 30 µm deformed layer and a 40 µm layer, is of secondary importance compared to the distinction between a 5 µm and 15 µm layer, as both of the thicker layers would likely be considered excessive and undesirable. As such, additional manufacturing process changes would be needed to bring this down to a more acceptable level.

The use of XRD-SIIM necessitates a level of health and safety considerations considering the use of ionising radiation. In this study, portable leaded acrylic radiation shielding was placed around the XRD hardware at the entrance of the machining centre to prevent line-of-sight access to the X-ray beam. The small penetration depth of low power X-rays used in XRD-SIIM means that the machine enclosure acts as an inherent radiation shield, with only several tens of microns of metal required to attenuate the X-rays. If an X-ray unit can be housed within the machining centre then no additional shielding would be required aside from at the windows.

Inspection depth can be tailored by employing different X-ray radiation due to differences in X-ray attenuation. Previous work [11] has shown, for example, that thin features such as white layers smaller than 5 µm can be detected more accurately by using a copper X-ray tube (4 µm penetration depth) compared to a Chromium or Manganese tube (>10 µm penetration depth). For thicker layers the opposite approach can be taken. By tailoring the X-ray radiation to the desired inspection range, accuracies of 0.5 µm – 2 µm have been achieved for white layers and deformed layers respectively. Ultimately, due to limitations on possible tube types, inspection depths beyond 20 µm are not currently possible on portable diffractometers, as such accurate sizing of such layers is not possible, instead they can only be identified as significantly deformed.

It is apparent, therefore, that XRD-SIIM significantly shortens the iterative cycle of testing and surface validation during the development of new processes, by offering results immediately post-cut. By removing the need to preserve numerous specimens for microscopy inspection at each down-selection step and reducing the long lead time for inspection

results down from weeks to minutes, inspection is no longer the rate-determining step. Additionally, the removal of the requirement for destructive sectioning reduces material waste, particularly in applications such as face turning where extracting specimens renders a large portion of the surface unusable for further turning trials.

The non-destructive nature of XRD-SIIM means the technique could also be applied in a production environment to maintain quality in production by enabling a Zero Defect approach to microstructural machined surface integrity inspection. The applicability of the method will depend on the nature of the component being manufactured and the level of validation required. For components with many inspection locations, inspection off-machine in a laboratory environment may be preferred, to maximise time spent machining. However, for situations where the throughput rate is less of a factor, e.g. components which may spend several days on a machine, inserting a short inspection cycle could be beneficial.

The process flow for implementing and then maintaining a machining operation from a microstructural surface integrity perspective is illustrated in Fig. 11 for validation via the industry-standard microscopy inspection method and Fig. 12 for a Zero Defect enabled process. It should be noted however that the application of XRD-SIIM for final certification of a new process for use in a production environment depends on the defined certification requirements of relevant authorities in different sectors. Hence, currently, the technique is best suited as a process development tool, to streamline the design of a new process without providing final certification.

On-machine XRD-SIIM combined with a zero defect approach to machined surface evaluation could lead to a step-change advancement in component validation due to improvements in timescales and a reduction in inventory needs. Validation results obtained via XRD-SIIM means that component quality information can be included in the digital passport of a component, immediately post-machining and these results can be carried forward into subsequent processes and potentially be used to inform the expected life in service. With microscopy inspection, the lead time is days or weeks for inspection results and the component is destroyed so there is no need to carry the information forward in a digital passport. Inspecting on-machine will also reduce waste by enabling re-work, for example by identifying anomalous surface generation behaviour before the final geometry is reached, allowing the manufacturing engineer to act and mitigate defect formation. The study has shown that XRD-SIIM could also reduce the reliance on tool wear assessments, as a deterioration in tool flank condition reflected in a deterioration in deformed layer thickness. However, full tool wear assessment should also consider measures beyond the flank wear, and further work is needed to verify any correlation to microstructural surface integrity and XRD-SIIM for wear types such as edge chipping for example.

Ultimately, with the concurrent development of closed-loop control algorithms for feedback control of the machining operation, it may be possible to implement in-cycle control of microstructural machining defects. This would unlock the full potential of zero defect machining by allowing machining processes to automatically return to conformance after defect generation is identified. Considering the opposite scenario, where the generated surface is well within desired limits, for example, due to the use of conservative fixed cutting conditions to significantly reduce the likelihood of defect generation, a zero defect compatible technique like XRD-SIIM could facilitate a move away from fixed machining processes. If assurances can be provided on the microstructural surface integrity state by direct measurements, manufacturing process limits such as tool life could be driven by defect formation or the lack thereof, maximising the resource utilisation during manufacture and thereby minimising waste.

5. Conclusions

This study has demonstrated, for the first time, on-machine non-destructive microstructural surface integrity inspection using XRD-SIIM.

- The technique can be used to generate surface integrity fingerprints of an operation, characterising the evolution of near-surface machining-induced plastic deformation throughout tool life.
- XRD-SIIM shows equivalence to cross-sectional microscopy microstructural for sizing of deformed layers up to the X-ray penetration depth, and whilst the sizing resolution deteriorates beyond 20 μm, the equipment can still identify that a thick deformed layer has formed.
- There are limitations with validating XRD-SIIM against microscopy, which is open to inspector interpretation. Future work should therefore look to undertake measurement systems analysis of XRD-SIIM and microscopy for inspection of microstructural surface integrity features, and seek to validate XRD-SIIM by an alternate quantitative approach such as microgrid distortion.
- By applying XRD-SIIM to the cutting process development challenges, different insert grades, coolant application methods and cutting parameters could be benchmarked with the non-destructive method enabling down-selection of the optimal process from a deformed layer perspective, alongside traditional metrics such as productivity and tool wear.
- By enabling microstructural surface integrity feedback at regular intervals through a machining operation, XRD-SIIM offers faster (same-day) process optimisation and provides additional information on the through-tool-life deformed layer evolution, which could be missed via start and end-of-cut microscopy assessment.
- With the removal of the need to preserve specimens for microscopy assessment, material waste from this mechanism can be eliminated.

Declaration of Competing Interest

The authors declare the following financial interests/personal relationships which may be considered as potential competing interests: Matthew Brown reports financial support and equipment, drugs, or supplies were provided by AB Sandvik Coromant. Matthew Brown reports equipment, drugs, or supplies was provided by Rolls-Royce plc. Matthew Brown, Pete Crawforth has patent #Non-destructive detection of surface and near surface abnormalities in a metallic product (US11815477B2) issued to University of Sheffield. If there are other authors, they declare that they have no known competing financial interests or personal relationships that could have appeared to influence

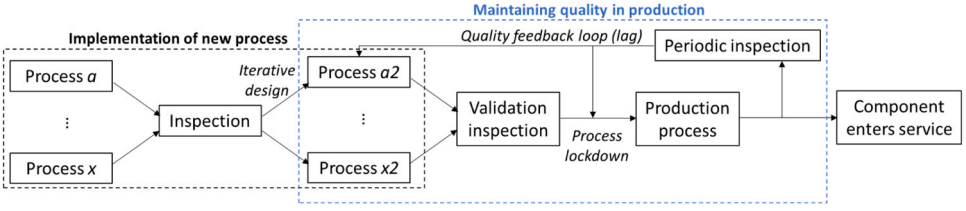

Fig. 11. A schematic representation of a traditional approach to new process implementation and subsequently business-as-usual production operations, where microstructural surface integrity can only be undertaken destructively, in a laboratory environment.

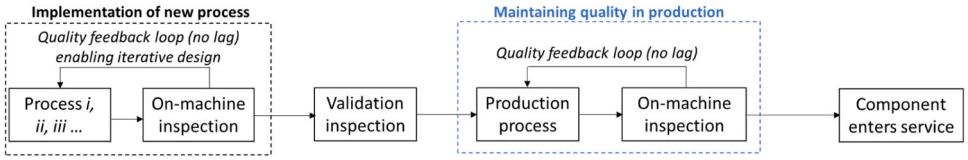

Fig. 12. A schematic representation of the zero defect approach to new process implementation where microstructural surface integrity inspection can be undertaken non-destructively on-machine.

the work reported in this paper.

Acknowledgements

This work was supported by High Value Manufacturing Catapult funding provided by Innovate UK in addition to funding provided by Sandvik Coromant. The tooling used in the study was provided by Sandvik Coromant and the authors wish to extend their thanks for the guidance and expertise offered throughout the study. The RR1000 material used in this study was supplied by Rolls-Royce PLC and the authors wish to extend thanks to them.

References

[1] Choudhury I, El-Baradie M. Machinability assessment of inconel 718 by factorial design of experiment coupled with response surface methodology. J Mater Process Technol 1999;vol. 95(1-3):30–9.
[2] Herbert C, Axinte DA, Hardy M, Withers P. Influence of surface anomalies following hole making operations on the fatigue performance for a nickel-based superalloy. J Manuf Sci Eng 2014;vol. 136(5):1–9. https://doi.org/10.1115/1.4027619.
[3] M'Saoubi R, Outeiro JC, Chandrasekaren H, Dillon Jr OW, Jawahir IS. A review of surface integrity in machining and its impact on functional performance and life of machined products. Int J Sustain Manuf 2008;vol. 1:203–36.
[4] Liao Z, et al. Surface integrity in metal machining-Part I: fundamentals of surface characteristics and formation mechanisms. Int J Mach Tools Manuf 2021;vol. 162:103687.
[5] Bushlya V, Zhou JM, Lenrick F, Avdovic P, Ståhl JE. Characterization of white layer generated when turning aged inconel 718. Procedia Eng 2011;vol. 19:60–6. https://doi.org/10.1016/j.proeng.2011.11.080.
[6] Brown M, et al. Quantitative characterization of machining-induced white layers in Ti–6Al–4V. Mater Sci Eng: A 2019;vol. 764:138220. https://doi.org/10.1016/j.msea.2019.138220.
[7] Attanasio A, Umbrello D, Cappellini C, Rotella G, M'Saoubi R. Tool wear effects on white and dark layer formation in hard turning of AISI 52100 steel. Wear 2012;vol. 286:98–107.
[8] Chou YL, Evans CJ. White layers and thermal modeling of hard turned surfaces. Int J Mach Tools Manuf 1999;vol. 39:1863–81.
[9] Uysal A, Altan E. Slip-line field modelling of rounded-edge cutting tool for orthogonal machining. Proc Inst Mech Eng, Part B: J Eng Manuf 2016;vol. 230(10):1925–41.
[10] Brown M, et al. Non-destructive detection of machining-induced white layers through grain size and crystallographic texture-sensitive methods. Mater Des 2021;vol. 200:109472.
[11] Brown M, Crawforth P, Curtis D. Rapid non-destructive sizing of microstructural surface integrity features using x-ray diffraction. NDT E Int 2022;vol. 131:102682.
[12] B.D. Cullity, *Elements of X-ray diffraction, Addison* (Wesley Mass). 1978.
[13] Naskar A, Paul S. Non-destructive measurement of grinding-induced deformation-depth using grazing incidence X-ray diffraction technique. NDT E Int 2022;vol. 126:102592.
[14] Kwong J, Axinte DA, Withers PJ. The sensitivity of Ni-based superalloy to hole making operations: Influence of process parameters on subsurface damage and residual stress. J Mater Process Technol 2009;vol. 209(8):3968–77. https://doi.org/10.1016/j.jmatprotec.
[15] Williamson G, Hall W. X-ray line broadening from filed aluminium and wolfram. Acta Metall 1953;vol. 1(1):22–31.
[16] Baumann G, Fecht H, Liebelt S. Formation of white-etching layers on rail treads. Wear 1996;vol. 191(1-2):133–40.
[17] Change IP o C. Global warming of 1.5° C: An IPCC special report on the impacts of global warming of 1.5° C above pre-industrial levels and related global greenhouse gas emission pathways, in the context of strengthening the global response to the threat of climate change, sustainable development, and efforts to eradicate poverty. Intergov Panel Clim Change 2018.
[18] Powell D, Magnanini MC, Colledani M, Myklebust O. Advancing zero defect manufacturing: A state-of-the-art perspective and future research directions. Comput Ind 2022;vol. 136:103596.
[19] Scherrer P. Bestimmung der Grosse und inneren Struktur von Kolloidteilchen mittels Rontgenstrahlen. Nach Ges Wiss Gottingen 1918;vol. 2:8–100.
[20] Stokes A, Wilson A. The diffraction of X rays by distorted crystal aggregates-I. Proc Phys Soc 1944;vol. 56(3):174.
[21] Cullity BD, Stock SR. Elements of X-ray Diffraction. New Jersey: Prentice hall,; 2001.
[22] Hubbell JH, Seltzer SM. Tables of X-ray mass attenuation coefficients and mass energy-absorption coefficients 1 keV to 20 MeV for elements Z= 1 to 92 and 48 additional substances of dosimetric interest, National Inst. of Standards and Technology-PL, Gaithersburg, MD (United States). Ioniz Radiat Div 1995.
[23] Ezugwu E, Wang Z, Machado A. The machinability of nickel-based alloys: a review. J Mater Process Technol 1999;vol. 86(1):1–16.